

Uduakobong Okorie<sup>1,2</sup>, Ubong Robert<sup>1\*</sup>, Sylvester Ekong<sup>1</sup>,  
Usenobong Akpan<sup>1</sup>, Ito Udo<sup>3</sup>

<sup>1</sup>Department of Physics, Akwalbom State University, Mkpato Enin, P.M.B. 1167, Nigeria, <sup>2</sup>Department of Physics, University of South Africa, Florida 1710, Johannesburg, South Africa, <sup>3</sup>Department of Chemistry, University of Uyo, Uyo, P.M.B. 1017, Nigeria

Scientific paper

ISSN 0351-9465, E-ISSN 2466-2585

<https://doi.org/10.62638/ZasMat1321>



Zastita Materijala 66 ( )  
(2025)

## Assessment of the properties of recycled oil palm leaflets and groundnut shells based composite panels

### ABSTRACT

*This study was designed to examine the feasibility of recycling groundnut shells and oil palm leaflets into materials suitable for structural applications. Groundnut shell particles (GSP) and oil palm leaflet particles (OLP) were prepared and mixed at varying proportions (0, 25, 50, 75, and 100 %) on dry weight basis to produce composite panels. The ratio by weight of the binder (topbond) to composite mix was 1:1. Three samples were produced per formulation, dried completely, and then subjected to various tests to determine their suitability for structural applications. The results showed that increase in the content of the OLP from 0 % to 100 % yielded average water absorption (61.85 - 86.83) %, thickness swelling (3.33 - 6.17) %, void fraction (4.51 - 9.22) %, bulk density (598.9 - 502.8) kgm<sup>-3</sup>, thermal conductivity (0.2129 - 0.2004) Wm<sup>-1</sup>K<sup>-1</sup>, specific heat capacity (1475 - 1886) Jkg<sup>-1</sup>K<sup>-1</sup>, thermal diffusivity (2.410 - 2.113) 10<sup>-7</sup>m<sup>2</sup>s<sup>-1</sup>, heat penetration time (4.426 - 5.048) mins, flexural strength (1.454 - 1.312) N/mm<sup>2</sup>, and modulus of elasticity (218.8 - 196.5) N/mm<sup>2</sup>. Screwability and nailability were 100 % without alteration. It was revealed that the GSP-OLP panels developed in this study could be used as promising alternatives to plywood, asbestos, plaster of Paris which are known conventional ceilings applied for thermal insulation in building design. They could as well be applied internally as wall partition materials. Relying on the oil palm leaflets and groundnut shells for such undertaking could enhance low-cost building construction and at the same time mitigate the adverse effects associated with their disposal.*

**Keywords:** Bulk density, ceiling, flexural strength, thermal insulation, waste materials

### 1. INTRODUCTION

Valorization of recyclable wastes is a viable and result-oriented strategy that can ensure the availability of eco-friendly, high-performance, and low-cost materials for structural applications. In the housing sector, the use of such materials is highly competitive among builders and architects for mitigation of global warming effects, thus highlighting the positive impact of this innovative approach to sustainable building construction. Also, the competitiveness noticed in the use of recyclable wastes indicates the fact that items of high economic value are discarded unknowingly [1] and this encourages intensification of efforts towards optimal utilization of the wastes for beneficial purposes.

Conversion of certain agro-industrial wastes into boards suitable for use, particularly, as ceiling and for partition materials in building construction has been successfully demonstrated in recent researches. Some of such novel ceilings include composite panels based on sugarcane bagasse [2], oil palm mesocarp fiber [3], coconut shells with waste papers [4], and tiger nut with waste cartons [5]. Findings on them have shown that they are capable of outperforming conventional ceilings such as asbestos, polyvinyl chloride (PVC), plywood, Isorel, and plaster of Paris (POP) as far as the need for thermal comfort is a priority. Studies have also shown that composites produced from corncob and waste ceramic tiles [6], sawdust, corncob and rice husks [7], sawdust and coconut fibers [8] are suitable for application as wall partition elements in building construction. As shelter (building) remains one of the basic needs of humans in the world, it is expected to be affordable and safe for use [9]. In this regard, one way of ensuring affordability and safety is through utilization of waste-derived products to carry out thermal insulation aspect of a building's structural

\*Corresponding author: Ubong Williams Robert

E-mail: ubresearch2017@gmail.com

Paper received: 18.12.2024

Paper corrected: 09.03. 2025.

Paper accepted: 20.03. 2025.

design. For such task, the knowledge of the materials' properties is very crucial while considering continuous construction opportunities. Since waste generation results from human activity and is certainly inevitable, this paradigm shift of focus via adoption of the 3 Rs (Reduce, Reuse, and Recycle) principle is a sure way to enhance sustainable development in any country [10].

Agriculture is a typical sector in which huge quantities of residues/wastes are generated (mostly during harvesting and processing operations). For example, harvesting of oil palm (*Elaeisguineensis*) fruits usually requires cutting of some of the palm fronds. A mature oil palm has 30 to 50 fronds [10] and its economic lifespan in plantations takes 25 to 30 years with the fruits available year-around [12]. Each palm frond is about 7 m long and it consists of a petiole which is 150 cm in length with a rachis bearing 250 to 350 leaflets (pinnae) each of which may be about 130 cm long [13]. As of 2019, the global oil palm plantation reached over 19.6 million hectares [14, 15]. Among the wastes associated with oil palm business, the leaflets are usually left in the field. Groundnut (*Arachishypogaea L.*) is another crop with high volume of waste generation, especially the shells which are usually discarded as wastes during processing. According to the 2023 Statistics from the Food and Agriculture Organization (FAO), groundnut production in the world reached 50.46 million metric tons, highlighting its significance as a major agricultural commodity. Sathiparan et al. [16] estimated annual worldwide quantity of groundnut shells to be 11 million metric tons. This enormous quantity of the bio-waste makes it remain under-utilized despite its use for biodiesel production [17], carbon nano-sheet formation [18], dye degradation [19], and production of paper [20]. It is observed that both the oil palm leaflets and groundnut shells have very high sustainability and are readily available. Unfortunately, they are prevalently subjected to open-air incineration as a way of their disposal. This practice, which is as a result of limited and ineffective solid waste management systems in less-developed and developing countries, is detrimental to the environment and public health [21, 22]. There is an urgent need to explore other safe options to mitigate the menace.

Therefore, the aim of this research is to utilize groundnut shells with oil palm leaflets in the development of composite panels for structural applications in buildings. Raju and Kumarappa [23] investigated the tensile strength, tensile modulus, modulus of rupture, and impact strength of groundnut shells particle-reinforced epoxy composites. They found that the composite would

be a substitute for wood-based material in many applications. Olamide et al. [24] characterized particleboards produced from groundnut shell and rice husk and found their modulus of elasticity and modulus of rupture to be 932.4 N/mm<sup>2</sup> and 3.50 N/mm<sup>2</sup> respectively, indicating that the particle boards met the American national Standard specification for general purpose particleboards. Jacob et al. [25] studied the effect of groundnut shell powder on the viscoelastic properties of recycled high density polyethylene composites. They observed that reinforcement with 25%wt groundnut shell powder yielded storage modulus of 1158.47 MPa against 1033.58 MPa recorded by unreinforced composites. Ferrández-García et al. [26] trimmed the leaflets from fronds of different palm tree species, developed particleboards and then evaluated the density, thickness swelling, water absorption, thermal conductivity, modulus of rupture, and modulus elasticity of the particle boards. The results showed that the manufactured particleboard had similar performance to conventional wood particleboard and good thermal insulation properties. Nyior et al. [27] examined the mechanical properties of raffia fiber/groundnut shell reinforced epoxy hybrid composites and found maximum tensile strength, modulus of rupture, modulus of elasticity, and impact strength of 9.56 MPa, 41.6 MPa, 4720 MPa, and 1.6 kJ/m<sup>2</sup> respectively. Considering these results, they concluded that the composite material could be alternatively used in automotive interior panels such as boot liner, side and door panels, rear storage shelf and roof cover. A study conducted by Mausam et al. [28] to examine the potentials of groundnut shell, sawdust, and hybrid bio-filler as reinforcement in epoxy matrix revealed that fiber treatment with Maleic acid was more effective in enhancing the flexural, tensile, and impact properties of the composite possibly due to synergetic impact in the treatment. Ekpenyong et al. [29] found that composite panels made from untreated and alkali-treated groundnut shells with cassava starch slurry as binding agent exhibited thermal conductivity, solar radiation absorptivity, and flexural strength of 0.1742 Wm<sup>-1</sup>K<sup>-1</sup>, 16.15 m<sup>-1</sup>, and 2.255 N/mm<sup>2</sup>. They concluded that such panels could outperform Isorel, asbestos, plaster of Paris, which are widely-used conventional ceilings in buildings.

In this research, relevant physical, thermal, and mechanical properties of the panels will be assessed in order to ascertain their suitability for the intended application. This paper will be the first to report on such scientific undertaking and it is hoped that findings from the research would be of immense benefits to researchers, waste managers, and manufacturers of building materials.

## 2. EXPERIMENTAL PART

### 2.1. Materials

Topbond (Model KW001 general purpose white glue having viscosity of 1600 cP), oil palm leaflets, and groundnut shells were among the materials used in this study. The topbond was procured from a building materials shop while both the oil palm leaflets and groundnut shells were gathered as waste materials. All the materials were sourced in large quantities within Uyo metropolis, Akwalbom State, Nigeria.

### 2.2. Processing and Analysis of the oil palm leaflets and groundnut shells

The oil palm leaflets and groundnut shells were immersed separately in water to remove any accompanying dirt/impurities from them. After 10 hours, they were removed from the water and exposed to sunlight, ensuring that their surfaces were dried before pulverizing them. Each pulverized material was sun-dried for several days until it became moisture-free. The material was then screened using a standard US sieve with openings measuring 2 mm in diameter, and the quantity that passed the sieve was utilized to prepare samples of the panel. Prior to the

fabrication of the samples, the screened materials were coded for ease of identification. Also, their loose density was evaluated as the ratio of mass to untapped volume [30] and the chemical composition of each of them was determined by adopting gravimetric method [31].

### 2.3. Preparation of the Samples

The topbond was applied as the binder in all the formulations adopted in this research. Table 1 shows the various mixes adopted to develop the test samples. In each case, the materials were proportioned by weight on dry basis, maintaining 1:1 ratio of the material mix to the binder. Three identical samples were considered for each mix design and all of them were compacted simultaneously with the aid of a laboratory-made compacting machine maintained at 5 kN for 10 hours.

Table 1. Mixes of the processed materials

Material	Proportion (%)					
GSP	0.0	25.0	50.0	75.0	100.0	
OLP	100.0	75.0	50.0	25.0	0.0	

GSP = Groundnut shell particles;

OLP = Oil palm leaflet particles



Figure 1. Samples preparation processes

For evaluation of the physical and thermal properties, the samples were prepared to diameter of 110 mm with thickness measuring 8 mm whereas the samples developed for assessment of mechanical properties were of dimensions 185 mm × 130 mm × 14 mm. Before the mixture was cast, the inner edges of the molds were properly covered with release agent (known as 8329-epoxy mold release) to ensure easy demolding. Drying of the samples was carried out under intense sunlight for several days until constant weight was achieved in each case, after which all the samples were subjected to the various tests intended for them in this study. Figure 1 summarizes some basic stages in the production of the samples.

## 2.4. Testing of the Samples

### 2.4.1. Physical properties

The bulk volume of each sample was determined by modified water displacement method, employing waste candle wax as the coating material [32]. Using a digital weighing (S. METTLER – 600/0.1g), the sample's mass was measured and then used in calculation of the sample's bulk density based on equation (1) [3, 33]

$$\rho = \frac{M_s}{V} \quad (1)$$

Where  $\rho$  = bulk density,  $M_s$  = mass of the sample under test, and  $V$  = bulk volume of the sample.

Assessment of the existence of voids in each sample was deemed necessary since the OLP and GSP are porous, particulate, and non-cohesive. In this research, void fraction of the samples was investigated with the aid of gas pycnometer (Model G-DenPyc 2900 GoldAPP Instrument) utilizing helium as described in [28]. The total volume of the void,  $V_a$  was obtained and used alongside the sample's volume,  $V$  to compute the void fraction,  $V_f$  using equation (2)

$$V_f = \left( \frac{V_a}{V} \right) 100\% \quad (2)$$

The test protocols documented in the ASTM D1037 [34] were applied to evaluate the water absorption and thickness swelling of the samples. In both cases, the samples were completely immersed in the water for 24 hours. All thickness measurements were performed by means of digital verniercalipers (0 -15 cm). Using the data gathered for the masses and thicknesses, the water absorption was computed based on equation (3) [2].

$$WA = \left( \frac{M_f - M_i}{M_i} \right) 100\% \quad (3)$$

where  $WA$  = water absorption,  $M_i$  = mass of the sample before the immersion, and  $M_f$  = mass of the sample after the immersion

The thickness swelling was similarly determined by calculation using equation (4)

$$T_s = \left( \frac{T_f - T_i}{T_i} \right) 100\% \quad (4)$$

Where  $T_s$  = sample's thickness swelling,  $T_i$  = thickness of the sample before the immersion, and  $T_f$  = thickness of the sample after the immersion.

### 2.4.2. Thermal properties

Each sample's thermal conductivity coefficient was examined using Modified Lee-Charlton's Disc Apparatus technique [35]. Figure 2 shows both the experimental and schematic features of the measurements setup as used in this research. The sample under test was inserted between the two identical discs and heat was supplied from the electric hotplate (Model E4102WH), ensuring that the thickness of the sample and that of the upper disc were properly lagged using cotton wool. When the steady state was reached, the temperatures of the two discs were noted. Then, the test sample was removed from the assembly and the upper disc was heated until its temperature rose to about 10°C above the value obtained at the steady state. After that, the heating was discontinued and the heat source was removed alongside the lower disc. With the sample placed on the upper disc, the temperature - time data were taken while the disc was cooling until its temperature dropped to about 10°C below the value obtained at the steady state. The data gathered were used to plot a cooling curve (a graph of cooling temperature against time) by employing Origin Software (Version 2019b) and then generate a model from which the required rate of cooling was determined using the principle of differentiation. From the various data gathered, the thermal conductivity was computed using equation (5) [36].

$$k = \left( \frac{Mcx}{A\Delta\theta} \right) \frac{dT}{dt} \quad (5)$$

Where  $k$  = thermal conductivity,  $M$  = mass of the disc,  $A$  = sample's cross-sectional area,  $c$  = specific heat capacity of the disc,  $x$  = thickness of the sample,  $\Delta\theta$  = difference in temperature between the cross-sectional surfaces of the sample, and  $\frac{dT}{dt}$  = rate of cooling of the disc.

The samples' specific heat capacity was determined by using mixture method of calorimetry [37]. In this study, copper calorimeter was employed with its stirrer as the measurement system. The calorimeter was filled with cold water to about two-third of its capacity, noting the mass of water and that of the calorimeter (with its stirrer). For the purpose of heating, a stainless steel was filled with dry sharp river-bed sand and the sample was embedded in the sand.

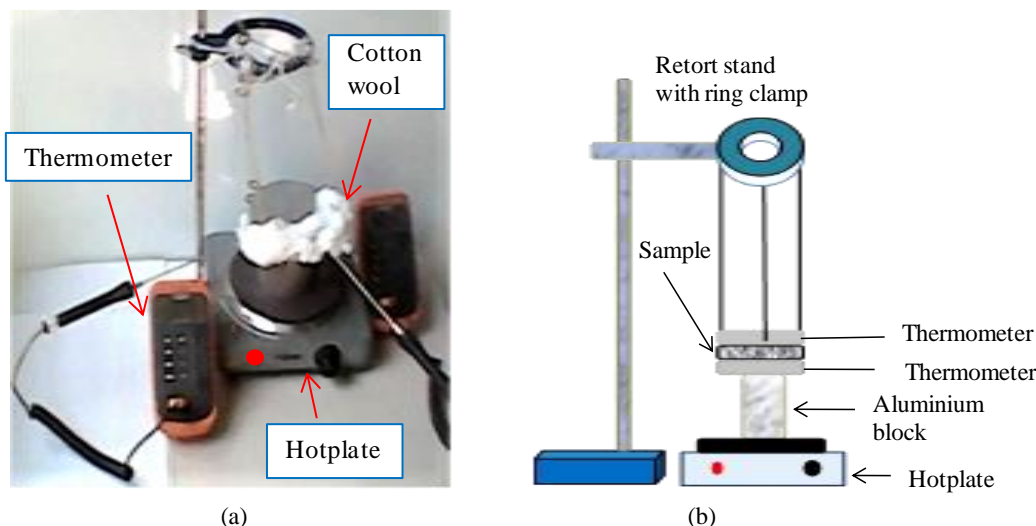


Figure 2. Setup for the thermal conductivity examination (a) Experimental (b) Schematic

The sample was embedded in such a way that it did not make any direct contact with the container. As the container was being heated, the temperature of the sand was measured using a copper-constantan thermocouple. When the temperature remained unchanged for about five minutes, the sample was removed and quickly transferred by tongs into the water in the calorimeter. The mixture was stirred gently until it attained thermal balance. With the assumption of heat energy conservation [36], the specific heat capacity,  $C$  of the investigated sample was obtained based on equation (6)

$$C = \left( \frac{Q_c + Q_w}{M_b \delta T} \right) \quad (6)$$

Where  $Q_c$  = quantity of heat gained by the calorimeter and its stirrer,  $Q_w$  = quantity of heat gained by water in the calorimeter,  $M_b$  = mass of the sample under test, and  $\delta T$  = change in temperature of the sample.

The bulk density, thermal conductivity, and specific heat capacity already obtained were applied to calculate the corresponding thermal diffusivity,  $\lambda$  for the sample using equation (7) [3, 38 – 40]

$$\lambda = \frac{k}{\rho C} \quad (7)$$

More so, the heat penetration time,  $t$  of each sample was obtained by calculation using equation (8) [41]

$$t = \frac{x^2}{\lambda} \quad (8)$$

#### 2.4.2. Mechanical properties

Since the successful application of some thermal insulation panels require the use of screw to fasten them, investigation of screwability was

considered a necessity in this study. The screw used in testing the samples was 4 mm thick and of length 40 mm with pitch of 2 mm. Assessment of the samples for screwability was performed in accordance with the procedure used in [31], in which case the screw was driven through the thickness of the sample under test until either it penetrated successfully or severely damaged the sample before the process was discontinued. Then, the screwability was obtained by applying equation (9)

$$S_b = \left( \frac{D}{x} \right) 100 \% \quad (9)$$

where  $S_b$  = screwability of the sample,  $D$  = distance penetrated by the screw, and  $x$  = thickness of the sample.

Evaluation of the samples' nailability was crucial in order to provide useful insights into the ability of each sample to withstand nailing during its application as a panel product. In performing this test on the samples, a carpenter's hammer and a 50mm nail were used [5]. As the nail was driven with hammer blow into each sample, the process was observed and stopped either after a successful penetration by the nailor when the sample developed a sign of visible crack. For a successful travel of the nail, the depth of nail penetration was same as the sample's thickness. But if a sign of crack was noticed, the depth of the nail penetration was determined as the difference between the nail's total length and the length of its remaining portion. The nailability was calculated using equation (10):

$$n_b = \frac{h}{x} \quad (10)$$

Where  $n_b$  = nailability of the sample,  $h$  = depth of nail penetration, and  $x$  = thickness of the sample.



The flexural strength and modulus of elasticity of the samples were tested in accordance with the procedure stipulated in ASTM D790 [42]. For each schedule of the test, three-point bending technique was applied after the sample had been placed on the flexure assembly of a Computerised Electromechanical Universal Testing Machine (WDW-10) and then loaded at the center of the support span with a test speed of 1mm/min. The deflection of the sample was taken per load until the sample failed to withstand the stress. Then, the maximum load was noted and used with the span length,  $L$ , width of the sample,  $b$ , and sample's thickness,  $x$  to calculate the flexural strength using equation (11)

$$\sigma = \frac{3PL}{2bx^2} \quad (11)$$

Where  $\sigma$  = flexural strength, and  $P$  = maximum load that caused the sample to fail flexurally.

Using the load and deflection data obtained, the flexural stress-deflection curve was produced and the slope of its linear portion was deduced for determination of the sample's modulus of elasticity based on equation (12)[22]

$$E = \frac{L^3 S_g}{4bx^3} \quad (12)$$

Where  $E$  = modulus of elasticity, and  $S_g$  = slope of the linear portion of the stress-deflection curve.

### 3. RESULTS AND DISCUSSION

#### 3.1. Properties of the GSP and OLP

Table 2 shows the properties of the processed materials (GSP and OLP) utilized in this study. It

Table 3. Physical properties of the samples

GSP:OLP (%)	WA (%)	$T_s$ (%)	$V_f$ (%)	$\rho$ ( $\text{kgm}^{-3}$ )
100:0	61.58 $\pm$ 0.08	3.33 $\pm$ 0.02	4.51 $\pm$ 0.02	598.9 $\pm$ 0.8
75:25	69.89 $\pm$ 0.06	3.72 $\pm$ 0.02	5.88 $\pm$ 0.02	570.6 $\pm$ 0.7
50:50	70.29 $\pm$ 0.09	4.87 $\pm$ 0.04	7.19 $\pm$ 0.03	561.2 $\pm$ 0.6
25:75	78.52 $\pm$ 0.08	5.79 $\pm$ 0.01	8.34 $\pm$ 0.02	512.9 $\pm$ 0.9
0:100	86.83 $\pm$ 0.04	6.17 $\pm$ 0.02	9.22 $\pm$ 0.04	502.8 $\pm$ 0.8

The thickness swelling of the samples relates positively with their water absorption. Shukla and Kamdem [44] observed a similar trend in their study on the properties of yellow-poplar (*Liriodendron tulipifera*) laminated veneer lumber. Also, some studies have revealed maximum thickness swelling of 19.34 %, 7.31 %, and 8.33 % for panels fabricated from pine tree bark [45], waste carton with Melon seed husks [22], and sugarcane bagasse with waste newspaper [2] respectively for structural applications. According to the European standard, the maximum thickness swelling values for 24-hour immersion stipulated for

can be seen that the GSP has greater loose density value than the OLP. Specifically, the difference in their loose densities is about 23.3 % with respect to the value obtained for the OLP. Though the lignin fractions are approximately the same in both cases, the OLP contains more cellulose and hemicelluloses compared to the GSP. These values signify that, chemically, the GSP and OLP cannot exhibit the same behavior.

Table 2. Properties of the GSP and OLP used

Parameters	Average value for five determinations	
Chemical composition:	GSP	OLP
Cellulose (%)	36.92	43.58
Hemicellulose (%)	26.89	36.16
Lignin (%)	19.58	19.65
Loose density ( $\text{kgm}^{-3}$ )	265.1	215.0

#### 3.2. Physical properties of the samples

From Table 3, it is clear that water absorption of the samples increases as the proportion of the OLP increases. This can be attributed to the fact that the OLP contains more hydrophilic constituents (cellulose and hemicelluloses), thereby exhibiting greater water uptake capability than the GSP. Akinyemi et al. [43] reported water absorption of 121.06 % for composite boards developed from corn cob and sawdust for indoor uses in buildings. Taking that into consideration, the GSP-OLP panels could be applied internally in building construction.

general purpose medium-density fiberboard with thickness of 6 mm to 9 mm for use in dry and under humid conditions are 17 % and 12 % respectively [46]. Based on these facts, all the GSP-OLP panel samples in this study have acceptable dimensional stability for interior applications even in moisture-prone regions.

Void fraction quantifies the empty spaces in the samples, providing insights into their pore geometry. The void fractions in this case show that the OLP has a greater tendency than the GSP to create voids in the resulting samples. Because of having lower loose density, continuous addition of

the OLP reduces the sample's bulk density. Meanwhile, the OLP creates more voids filled by air, thus leading to reduction in the sample's bulk density as its proportion increases. Increase in the content of the OLP from 0 % to 100 % decreases the bulk density of the samples by 16.0 %. Conventional ceilings such as plywood, asbestos, and plaster of Paris have bulk density of  $598 \text{ kgm}^{-3}$ ,  $1844 \text{ kgm}^{-3}$ , and  $1487 \text{ kgm}^{-3}$  respectively [31]. Comparatively, the highest bulk density obtained in this study is lower than the value for any of the mentioned ceilings. Thus, it can be deciphered that the samples could serve as promising substitutes to the conventional ceilings in building construction. Adoption of such undertaking is capable of reducing the dead loads, a situation that is highly desirable in buildings.

### 3.3. Thermal properties of the samples

The results showing heat transfer characteristics of the samples are presented in Table 4. It can be posited that decrease in thermal conductivity with increasing contents of the OLP is due to the possibility of the OLP to create more voids in the developed samples. Understandably, the voids are filled by air (which is a good thermal insulant), thus enabling the samples to restrict heat transmission the more as the OLP proportion increases. For building construction materials, thermal conductivity values are expected to range from  $0.023 \text{ Wm}^{-1}\text{K}^{-1}$  to  $2.900 \text{ Wm}^{-1}\text{K}^{-1}$  [47]. This means that the samples in this study are suitable for building design as far as efficient heat insulation is a necessary consideration for their application.

Table 4. Thermal properties of the samples

GSP:OLP (%)	$k \text{ (Wm}^{-1}\text{K}^{-1}\text{)}$	$C \text{ (10}^3\text{Jkg}^{-1}\text{K}^{-1}\text{)}$	$\lambda \text{ (10}^{-7}\text{m}^2\text{s}^{-1}\text{)}$	$t_p \text{ (mins)}$
100:0	$0.2129 \pm 0.0003$	$1.475 \pm 0.002$	$2.410 \pm 0.003$	$4.426 \pm 0.005$
75:25	$0.2101 \pm 0.0002$	$1.592 \pm 0.002$	$2.313 \pm 0.004$	$4.612 \pm 0.007$
50:50	$0.2083 \pm 0.0003$	$1.641 \pm 0.003$	$2.262 \pm 0.005$	$4.716 \pm 0.011$
25:75	$0.2026 \pm 0.0002$	$1.768 \pm 0.003$	$2.235 \pm 0.001$	$4.773 \pm 0.002$
0:100	$0.2004 \pm 0.0002$	$1.886 \pm 0.002$	$2.113 \pm 0.006$	$5.048 \pm 0.004$

The specific heat capacity of the samples are greater than the value of  $909.1 \text{ Jkg}^{-1}\text{K}^{-1}$  reported by Ezenwa et al. [48] for ceiling panels produced from breadfruit seed coat with low-density polyethylene as binder. By utilizing at least 75 % of the OLP, the specific heat capacity of the resulting samples exceeds the highest value of  $1686 \text{ Jkg}^{-1}\text{K}^{-1}$  obtained by Czajkowski et al. [49] for straw-based insulating panels recommended for building

engineering. These observations signify that the samples have greater potentials for efficient thermal insulation. Figure 3 depicts how the specific heat capacity and thermal diffusivity of the samples vary with the percentage of the OLP used in the samples. It is evident from the figure that the specific heat capacity increases whereas thermal diffusivity decreases as the content of the OLP increases.

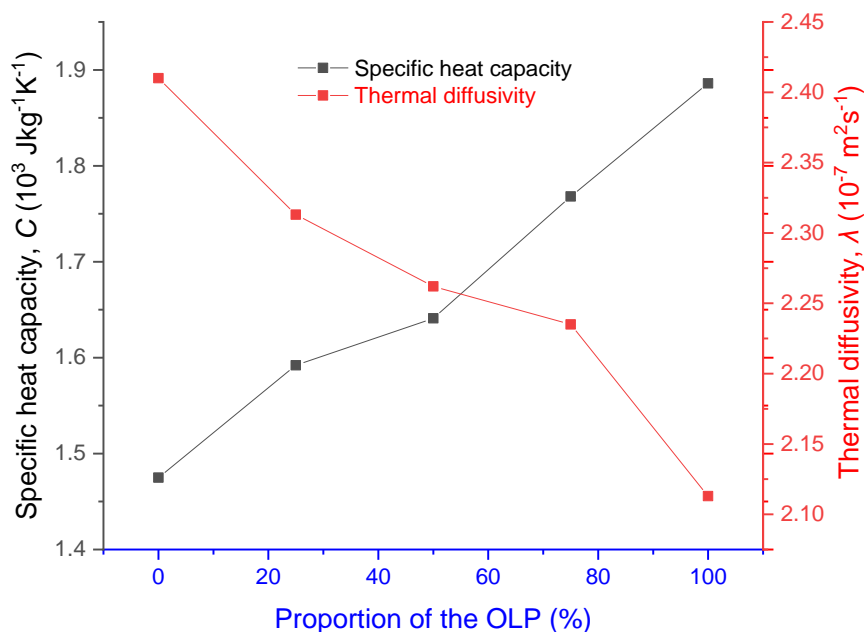


Figure 3. Variation of specific heat capacity and thermal diffusivity with OLP proportion

Since thermal diffusivity depends on specific heat capacity, it can be understood that higher capacity for heat storage enables delay in the spread of the absorbed thermal energy thereby reducing thermal diffusivity. With this situation, thermal insulation efficiency of the samples is enhanced and one consequence of such enhancement is the elongation of heat penetration time of the samples. Meanwhile, as the specific heat capacity increases, the rate of heat diffusion within the samples is reduced thus requiring more time for the thermal disturbance to diffuse and propagate temperature from one side of the samples to the other. Based on the obtained results in this case, the heat penetration time increases by 14.1 % due to variation in the content of the OLP from 0 % to 100 %.

The mechanical properties obtained for the samples are recorded in Table 5. Notwithstanding the mix design adopted in the study, the screwability and nailability of the samples remain 100 %. This simply implies that, in the course of their application, the samples can be screwed or nailed successfully. It is interesting to note that

voids increase with increasing proportions of the OLP in the samples. As such, the interfacial bonding between the constituent materials and binding agent is weakened as the percentage of the OLP increases, thus resulting to reduction in flexural strength of the samples.

However, the least flexural strength value in this case exceeds the maximum value of 0.1 N/mm<sup>2</sup> reported by Isheni et al [50] for composite ceiling boards developed from arbitrary mixtures of rice hush, maize husk, and saw dust with top gum as binder. Perhaps, this is due to the degree of adhesion the roughness of the GSP and OLP surfaces allow in the adhesive (topbond). In the case of modulus of elasticity, the results indicate a progressive decline in the resistance against deformation force as the OLP content increases. This means that the adhesion efficiency is increased more with the GSP than OLP at their similar levels of utilization in the composite mixes. Based on the results of the mechanical tests in this study, it is obvious that the GSP-OLP panels can be applied as interior partition materials as well as insulation ceilings in building construction.

*Table 5. Mechanical properties of the samples*

GSP:OLP (%)	$S_c$ (%)	$n_b$ (%)	$\sigma$ (N/mm <sup>2</sup> )	$E$ (N/mm <sup>2</sup> )
100:0	100.0 ± 0.0	100.0 ± 0.0	1.454 ± 0.004	218.8 ± 0.3
75:25	100.0 ± 0.0	100.0 ± 0.0	1.426 ± 0.003	212.3 ± 0.2
50:50	100.0 ± 0.0	100.0 ± 0.0	1.374 ± 0.003	205.8 ± 0.2
25:75	100.0 ± 0.0	100.0 ± 0.0	1.358 ± 0.002	200.9 ± 0.2
0:100	100.0 ± 0.0	100.0 ± 0.0	1.312 ± 0.002	196.5 ± 0.3

#### 4. CONCLUSION

The results of the investigations conducted in this study showed that the GSP-OLP panel samples recorded low bulk densities (502.8 kgm<sup>-3</sup> to 598.9 kgm<sup>-3</sup>) making them preferable to conventional ceilings like asbestos (1844 kgm<sup>-3</sup>) and plaster of Paris (1487 kgm<sup>-3</sup>) for reduction of dead loads in buildings. By using 100% GSP, the sample's thickness swelling (3.33%) was found to be less than that of the counterpart OLP-sample (6.17%), showing that the GSP is better for promoting dimensional stability. At 100% level of the OLP utilization, the sample's thermal conductivity was 5.87 % lower compared to the case with the GSP at similar loading level, thus indicating that the OLP is more potent in terms of improvement of thermal insulation efficiency in the samples. The GSP was found to be better than the OLP for promoting dimensional stability but less potent compared to the OLP in terms of improvement of thermal insulation efficiency in the samples. Due to their substantially high water absorption (ranging from 61.58% to 86.83%), the samples are suitable

for interior application only either as ceilings or wall partition materials. A mix of 25 % GSP and 75 % OLP yielded composite panel with balanced property, giving rise to lightweight board that could reasonably reduce dead loads and also possess enough strength to resist bending force during its service life. It could be adjudged that the GSP and OLP are suitable candidates for production of composite panels.

#### 5. REFERENCES

- [1] S.E. Etuk, U.W. Robert, J.B. Emah, O.E. Agbasi (2020) Dielectric Properties of Eggshell Membrane of Some Select Bird Species. *Arabian Journal for Science and Engineering*, 15(2), 91-98. <https://doi.org/10.1007/s13369-020-04931-7>
- [2] S.E. Etuk, U.W. Robert, O.E. Agbasi, N.J. Inyang (2023) Evaluation of Thermophysical and Strength Properties of Composite Panels Produced from Sugarcane Bagasse and Waste Newspapers. *Advances in Materials Science*, 23(1), 19 – 31. <https://doi.org/10.2478/adms-2023-0002>
- [3] A.U. Anonaba, F.C. Eze, I.C. Ndukwe (2024) Influence of Oil Palm Mesocarp Fiber on Physical



- Properties of fabricated plaster of Paris Ceilings. *Engineering and Technology Journal*, 42(4), 398-406  
<http://doi.org/10.0000.v8i2>
- [4] J. Dirisu, O.S.I. Fayomi, S.O. Oyedepo, E.T. Akinlabi (2019) A Preliminary study on chemical and physical properties of coconut shell powder as an enhancer in building ceilings for construction industry: Review. *IOP Conference Series Materials Sciences and Engineering*, 640, 012063.  
<https://doi.org/10.1088/1757-899X/640/1/012063>
- [5] U.S. Okorie, U.W. Robert, U.A. Iboh, G.P. Umoren (2020) Assessment of the suitability of tiger nut fiber for structural applications. *Journal of Renewable Energy and Mechanics*, 3(1), 32 – 39.  
[https://doi.org/10.25299/rem.2020.vol3\(01\).4417](https://doi.org/10.25299/rem.2020.vol3(01).4417)
- [6] O.J. Aladegboye, O.J. Oyedepo, T.J. Awolola, O.D. Oguntayo, O.Y. Babatunde, O.T. Ilesanmi, P.P. Ikubanni (2024) Physicomechanical and thermal properties of particleboard produced using waste ceramic materials and corncob. *Advances in Materials Science and Engineering*, 1, 8839814.  
<https://doi.org/10.1155/2024/8839814>
- [7] B.B. Hassan (2019) Production and characterization of particleboards from common agro-wastes in Nigeria. *International Journal of Innovative Science and Research Technology*, 4(1), 637 - 642
- [8] D.N. Tawasil, E. Aminudin, N.H.A.S. Lim, N.M.Z.N. Soh, P.C. Leng, G.H.T. Ling, M.H. Ahmad (2021) Coconut fiber and saw dust as green building materials: A laboratory assessment on physical and mechanical properties of particleboards. *Buildings*, 11(6), 256.  
<https://doi.org/10.3390/buildings11060256>
- [9] U.W. Robert, S.E. Etuk, O.E. Agbasi, U.S. Okorie, A. Lashin (2021) Hygrothermal properties of Environmental Technology & sandcrete blocks produced with raw and hydrothermally-treated sawdust as partial substitution materials for sand. *Journal of King Saud University – Engineering Sciences*. In Press  
<https://doi.org/10.1016/j.jksues.2021.10.005>
- [10] U.W. Robert, S.E. Etuk, O.E. Agbasi, G.P. Umoren, N.J. Inyang (2021) Investigation of thermophysical and mechanical properties of board produced from coconut (*Cocosnucifera*) leaflet. *Innovation*, 24, 101869. <https://doi.org/10.1016/j.eti.2021/101869>
- [11] Y.Y. Teng (2023) Oil palm anatomy: 5 ways an oil palm differs from a typical tree.
- [12] E. Barcelos, S. Rios, R.N. Cunha, R. Lopes, S.Y. Motoike, E. Babiychuk, A. Skirycz, S. Kushnir (2015) Oil palm natural diversity and the potential for yield improvement. *Front. Plant. Sci.*, 6, Article 190, 1 – 16.  
<http://doi.org/10.3389/fpls.2015.00190>
- [13] [13]K.P. P. Nair (2010) Oil Palm (*Elaeisguineensis*). In: *The Agronomy and Economy of important tree crops of the Developing World.*, p. 209 – 236.  
<https://doi.org/10.1016/B978-0-12-384677-8.00007-2>
- [14] A. Descals, S. Wich, E. Meijaard, Z. Szantoi (2021) High-resolution global map of smallholder and industrial closed-canopy oil palm plantation. *Earth System Science Data*, 13(3), 1211 - 1231
- [15] Z. Du, L. Yu, J. Yang, Y. Xu, B. Chen, S. Peng, T. Zhang, H. Fu, N. Harris, P. Gong (2022) A global map of planting years of plantations. *Scientific Data*, 9(1), 1 – 9.  
<https://doi.org/10.1038/s41597-022-01260-2>
- [16] N. Sathiparan, A. Anburuvel, v.V.Selvam, P.A. Vithurshan, (2023). Potential use of groundnut shell ash in sustainable stabilized earth blocks. *Constr Build Mater.*, 393, 132058.  
<https://doi.org/10.1016/j.conbuildmat.2023.132058>
- [17] B.AUdeh (2018) Bio-waste transesterification alternative for biodiesel production: a combined manipulation of lipase enzyme action and lignocellulosic fermented ethanol. *Asian Journal of Biotechnology Bioresource Technology*, 3(3), 1– 9.
- [18] N. Kanokon, S. Andrea, B. Peter (2018) Influence of KOH on the carbon nanostructure of peanut shell. *Resolution and Discovery*, 3(2), 29 – 32.
- [19] U.Z. Zakariyya, S.I. Saifullahi (2018) Evaluation of microcrystalline cellulose from groundnut shell for the removal of crystal violet and methylene blue. *Nanosci.Nanotechnol.* 8 (1), 1 – 6.
- [20] K. Upendra, T. Akshay, H. Vedika, K. Dhanashree, S. Prathamesh, N. Vivek (2018) Production of paper from Groundnuts shell. *Int. J. Adv. Res. Sci. Eng.*, 7 (2), 288 – 293.
- [21] J.B. Emah, A.A. Edema, S.A. Ekong, D.A. Oyegoke, U.W. Robert, F.O. Fasuyi (2024) Thermophysical, Strength, and Electrical Properties of Clay Modified with Groundnut Shell Ash for Building Purposes. *Journal of Sustainable Construction Materials and Technologies*, 9(4), 335 – 345.  
<https://doi.org/10.47481/jscmt.1600562>
- [22] U.W. Robert, S.E. Etuk, O.E. Agbasi, S.A. Ekong, E.U. Nathaniel, A.U. Anonaba, L.A. Nnana (2021) Valorization of Waste Carton Paper, Melon Seed Husks, and Groundnut Shells to Thermal Insulation Panels for Structural Applications. *Polytechnica*. 4(1), 97 – 106.  
<https://doi.org/10.1007/s41050-021-00034-w>
- [23] G.U. Raju, S. Kumarappa (2011) Experimental study on mechanical properties of groundnut shell particle-reinforced epoxy composites. *Journal of Reinforced Plastics and Composites*, 30(12), 1029 – 1037. <https://doi.org/10.1177/0731684411410761>
- [24] O. Olamide, A. Banjo, A.F. Omojo (2020) Optimization and material characterization of groundnut shell and rice husk for Production of particleboard. *ActaTecnología - International Scientific Journal about Technologies*, 6(3), 59 – 67.  
<https://doi.org/10.22306/atec.v6i3.78>
- [25] C. Ferrández-García, A.Ferrández-García, M.Ferrández-Villena, J.F. Hidalgo-Cordero, T. García-Ortuño, M.Ferrández-García (2018) Physical and Mechanical properties of particleboard made from palm tree prunings. *Forests*, 9(12), 755.  
<https://doi.org/10.3390/f9120755>
- [26] J. Jacob, P.A.Mamza, A.S. Ahmed, S.A. Yaro (2018) Effect of groundnut shell powder on the

- viscoelastic properties of recycled high density polyethylene composites. *Bayero Journal of Pure and Applied Sciences*, 11(1), 139 – 144
- [27] G. Nyior, S. Aye, S. Tile (2018) Study of mechanical properties of raffia palm fiber/groundnut shell reinforced epoxy hybrid composites. *Journal of Minerals and Materials Characterization and Engineering*, 6, 179 - 192.  
<https://doi.org/10.4236/jmmce.2018.62013>
- [28] K. Mausam, A. Bhardwaj, R.P. Singh (2021) Investigation of mechanical property of eco-friendly natural filler (groundnut, saw dust, and hybrid shell) reinforced epoxy based composite. *IOP Conference Series: Material Science and Engineering*, 1116, 012032.  
<https://doi.org/10.1088/1757-899X/1116/1/012032>
- [29] N.E. Ekpenyong, S.A. Ekong, E.U. Nathaniel, J.E. Thomas, U.S. Okorie, U.W. Robert, I.A. Akpabio, N.U. Ekanem (2023) Thermal Response and Mechanical Properties of Groundnut Shells' Composite Boards. *Researchers Journal of Science and Technology*, 3(1), 42 – 57.
- [30] U.W. Robert, S.E. Etuk, O.E. Agbasi, U.S. Okorie, Z.T. Abdulrazzaq, A.U. Anonaba, O.T. Ojo (2021) On the hygrothermal properties of sandcrete blocks produced with sawdust as partial replacement of sand. *Journal of the Mechanical Behavior of Materials*, 30(1), 144 – 155.  
<https://doi.org/10.1515/jmbm-2021-0015>
- [31] U.W. Robert, S.E. Etuk, O.E. Agbasi, P.D. Ambrose (2024) Development of Lightweight Sawdust-based Composite panels for Building Purposes. *International Journal of Lightweight Materials and Manufacture*, 7(5), 631 – 640.  
<https://doi.org/10.1016/j.ijlmm.2024.05.005>
- [32] U.W. Robert, S.E. Etuk, O.E. Agbasi (2019) Bulk Volume Determination by Modified Water Displacement Method. *Iraqi Journal of Science*, 60(8), 1704 – 1710.  
<https://doi.org/10.24996/ij.2019.60.8.7>
- [33] S.E. Etuk, U.W. Robert, O.E. Agbasi (2021) Investigation of heat transfer and mechanical properties of *Saccharum Officinarum* leaf boards. *International Journal of Energy and Water Resources*, 6(1), 05 – 102.  
<https://doi.org/10.1007/s42108-021-00123-7>
- [34] ASTM D 1037 (2020) Standard test methods for evaluating properties of wood-base fiber and particle panel materials. ASTM International, West Conshohocken, PA.
- [35] U.W. Robert, S.E. Etuk, O.E. Agbasi, U.S. Okorie, N.E. Ekpenyong, A.U. Anonaba (2022) On the Modification of Lee – Charlton's Disc Apparatus Technique for Thermal Conductivity Determination. *Researchers' Journal of Science and Technology*, 2(3), 1 – 17.  
<https://rejoist.com.ng/index.php/home/article/view/36>
- [36] U.W. Robert, S.E. Etuk, O.E. Agbasi, U.S. Okorie (2021) Quick Determination of Thermal Conductivity of Thermal Insulators Using a Modified Lee – Charlton's Disc Apparatus Technique. *International Journal of Thermophysics*, 42, 113  
<https://doi.org/10.1007/s10765-021-02864-3>
- [37] U.W. Robert, S.E. Etuk, U.A. Iboh, G.P. Umoren, O.E. Agbasi, Z.T. Abdulrazzaq (2020) Thermal and Mechanical properties of fabricated Plaster of Paris filled with groundnut seed coat and waste newspaper materials for structural application. *Építőanyag-Journal of Silicate Based and Composite Materials*, 72(2), 72 – 78.  
<https://doi.org/10.14382/epitoanyag-jsbcm.2020.12>
- [38] G.P. Umoren, A.O. Udo, I.E. Udo (2023) Suitability of *Lagenariabreviflora* Rind filled plaster of Paris ceilings for building design. *Researchers' Journal of Science and Technology*, 3, 1 – 14.  
<https://rejoist.com.ng/index.php/home/article/view/54>
- [39] S.E. Etuk, U.W. Robert, O.E. Agbasi (2022) Thermophysical properties of oil empty fruit bunch peduncle for use as a mulching material. *Journal of Oil Palm Research*, 35(3), 448 – 455.  
<https://doi.org/10.21894/jopr.2022.0065>
- [40] U.W. Robert, S.E. Etuk, O.E. Agbasi, G.P. Umoren (2020) Comparison of clay soils of different colors existing under the same conditions in a location. *Imam Journal of Applied Sciences*, 5; 68–73.  
[https://doi.org/10.4103/ijas.ijas\\_35\\_19](https://doi.org/10.4103/ijas.ijas_35_19)
- [41] U.W. Robert, S.E. Etuk, O.E. Agbasi, S.A. Ekong, Z.T. Abdulrazzaq, A.U. Anonaba (2021) Investigation of Thermal and Strength Properties of Composite Panels fabricated with Plaster of Paris for Insulation in Buildings. *International Journal of Thermophysics*, 42(2), 1 – 18.  
<https://doi.org/10.1007/s10765-020-02780-y>
- [42] ASTM D790 (2017) Standard Test Methods for Flexural Properties of Unreinforced and Reinforced Plastics and Electrical Insulating Materials. ASTM International, West Conshohocken, PA.
- [43] A.B. Akinyemi, J.O. Afolayan, E.O. Oluwatobi (2016) Some Properties of Composite Corn Cob and Sawdust particleboards. *Construction and Building Materials*, 127, 436 – 441.  
<https://dx.doi.org/10.1016/j.conbuildmat.2016.10.040>
- [44] S.R. Shukla, D.P. Kamdem (2009) Properties of laboratory made yellow-poplar (*Liriodendron tulipifera*) laminated veneer lumber: effect of adhesives. *European Journal of Wood and Wood Products*, 67(4), 397 – 406
- [45] İ. Özlüsoylu, A. İstek (2019) The Effect of Hybrid Resin Usage on Thermal Conductivity in Ecological Insulation Panel Production, 4th International Conference on Engineering Technology and Applied Sciences (ICETAS) April 24-28 2019 Kiev Ukraine. p. 292 – 296
- [46] BS EN 622 - 5 (2009) British Standard. Fiberboards - specifications Part 5.
- [47] E.R.K. Rajput (2015) Heat and mass transfer, 6<sup>th</sup> Revised edn., S. Chand and Company PVT Ltd, Ram Nagar, New Delhi, p.15
- [48] O.N. Ezenwa, E.N. Obika, I.E. Ekengwu, O.C. Okafor (2023) Thermal behavior of agro-waste based ceiling board and its filler material. *Journal of Research in Mechanical Engineering*, 9(1), 11 - 18.  
<https://doi.org/10.21203/rs.3.rs-2392145/v1>

- [49] L. Czajkowski, R. Kocewicz, J. Weres, W. Olek (2022) Estimation of thermal properties of straw-based insulating panels. *Materials*, 15(3), 1073. <https://doi.org/10.3390/ma15031073>
- [50] Y. Sheni, B.S. Yahaya, M.A. Mbishida, F. Achema, G.S. Karfe (2017) Production of agro waste composite ceiling board (A case study of the Mechanical properties). *Journal of Scientific and Engineering Research*, 4(6), 208 – 212.

## IZVOD

### PROCENA SVOJSTVA KOMPOZITNIH PLOČA NA BAZI RECIKLIRANOG PALMINOG ULJA I LJUSKE KIKIRIKIJA

Ova studija je osmišljena da ispita izvodljivost recikliranja ljuske kikirikija i otpadaka uljane palme u materijale pogodne za konstrukcijske primene. Čestice ljuske kikirikija (GSP) i čestice listova uljane palme (OLP) su pripremljene i pomešane u različitim proporcijama (0, 25, 50, 75 i 100 %) na osnovu suve težine da bi se dobile kompozitne ploče. Odnos mase veziva (topbond) prema kompozitnoj mešavini bio je 1:1. Proizvedena su tri uzorka po formulaciji, potpuno osušena, a zatim podvrgnuta različitim testovima da bi se utvrdila njihova pogodnost za strukturalne primene. Rezultati su pokazali da povećanje sadržaja OLP-a od 0 % do 100 % daje prosečnu apsorpciju vode (61, 85 - 86,83) %, debljinu bubrenja (3,33 - 6,17) %, udeo šupljina (4,51 - 9,22) %, toplotnu provodljivost 9 - 590 - 838. (0,2129-0,2004)  $\text{Vm}^{-1}\text{K}^{-1}$ , specifični toplotni kapacitet (1475–1886)  $\text{Jkg}^{-1}\text{K}^{-1}$ , toplotna difuzivnost (2,410 - 2,113)  $10^{-7} \text{ m}^2\text{s}^{-1}$ , vreme prodiranja toplote (4,426 - 5,045 min - 5,045 savijanja)  $\text{N/mm}^2$ , i modul elastičnosti (218,8 - 196,5)  $\text{N/mm}^2$ . Mogućnost uvrtnja i zakucavanja su 100% bez izmena. Otkriveno je da se GSP-OLP paneli razvijeni u ovoj studiji mogu koristiti kao obećavajuća alternativa šperploči, azbestu, gipsu iz Pariza koji su poznati konvencionalni plafoni koji se primenjuju za toplotnu izolaciju u projektovanju zgrada. Mogu se primeniti i unutra kao materijali za zidne pregrade. Oslanjanje na letke od uljane palme i ljuske kikirikija za takav poduhvat moglo bi poboljšati jeftinu izgradnju zgrada i istovremeno ublažiti štetne efekte povezane sa njihovim odlaganjem.

**Ključnereči:** Zapreminska gustina, plafon, čvrstoća na savijanje, toplotna izolacija, otpadni materijali

Naučni rad

Rad primljen: 18.12.2024.

Rad korigovan: 09.03.2025.

Rad prihvaćen: 20.03.2025.

Uduakobong Okorie  
Ubong Robert  
Sylvester Ekong  
Usenobong Akpan  
Itoro Udo

<https://orcid.org/0000-0002-4747-6298>  
<https://orcid.org/0000-0001-9979-7176>  
<https://orcid.org/0000-0003-0361-6575>  
<https://orcid.org/0009-0006-3026-8579>  
<https://orcid.org/0000-0002-5789-3132>